

Optimal Arrangement of Finite Element Loop Arrays for Parallel Imaging in a Spherical Geometry at 9.4 T

Andreas Pfommer¹ and Anke Henning^{1,2}

¹Max Planck Institute for Biological Cybernetics, Tuebingen, Germany, ²Institute for Biomedical Engineering, UZH and ETH Zurich, Zurich, Switzerland

Introduction: The limiting factor for parallel imaging (PI) [1-3] is the decrease in signal-to-noise ratio (SNR) which is proportional to $1/(g\sqrt{\chi})$, where χ accounts for reduced intrinsic signal averaging due to k-space undersampling and g is the geometry factor of the array. There have been several approaches in the past for optimizing finite element receiver arrays [4,5], the first by numerically distributing N loops by treating their centers as point charges and minimizing their Coulomb energy and the last by optimizing SNR at a specific voxel position. The purpose of this work was to find an optimal finite array configuration that minimizes the maximum g-factor in a given region of interest (ROI) and for given phase encoding directions.

Methods: To solve the electromagnetic field problem analytically the framework of dyadic Green's functions in spherically multilayered media [6] was used. Three layers were identified: The first layer (outermost) modelled the RF shield and ended at a radius of 162 mm completely filled with perfect electric conducting material (PEC). In the second layer (vacuum) at a distance of 122 mm to the origin, a set of N circular surface coils (PEC), all with the same radius R, were distributed. The third layer modelled the human head; based on average electromagnetic properties for gray and white matter at 9.4 T the following values were chosen: $\epsilon_r = 49.8$, conductivity = 0.59 S/m and radius of 92 mm. The fields were only calculated inside the "head", as this layer was chosen to be the ROI. The optimization problem was defined as:

$$\min_{\alpha, \beta, R} \max_{i \in \text{head}} \sqrt{\left[\left((S^H \Psi^{-1} S)^{-1} \right)_{i,i} (S^H \Psi^{-1} S)_{i,i} \right]} \quad (1)$$

The vectors α and β represent Euler angles that describe the position of each coil (s. fig 1). The matrices S and Ψ refer to the receive sensitivity and noise covariance of the loop array respectively. Phase encoding and related acceleration by parallel imaging was chosen to be in x and y direction. Here important to notice is the fact that the maximum g-factor was evaluated in the three-dimensional head volume. Therefore the coil arrangement was not meant to be optimal for a specific slice position but we ensured that for all slices in a plane $z = \text{const}$, the g-factor never exceeded a maximum value g_{\max} . The optimization was done in three steps: First N circular loops were distributed on the surface of a sphere with a radius of 122 mm by maximizing their minimal distance (s. Tammes problem [7]). In a second optimization step all loop elements were rotated by a common Euler rotation to get the best alignment regarding the acceleration directions. Finally the positions of the loops were kept fixed and the radius R was varied between $0.8 R_{\text{Tammes}}$ and the maximum possible loop radius of 122 mm to check whether separating or overlapping loops would decrease the maximum g-factor. All calculations were done in custom written MATLAB (The Mathworks, Natick, USA) code. The field expansion order l of the vector spherical harmonics was set to 30 being a trade-off between accuracy and simulation time. The calculation of the receive sensitivities was performed on a 3D Cartesian grid with isotropic resolution of 3.8 mm. The min-max optimization problem in the second and third step was solved with MATLAB's "fminimax" function. To prevent the algorithm running into local minima a sweep through the parameter space was done prior to the optimization to find suitable starting values.

Results: Figure 2 shows the optimal arrangement for 8, 16 and 32 circular surface coils minimizing the maximum value of the g-factor for 2x2, 3x3 and 4x4 undersampling in x and y direction. For all cases the optimization of the loop radius did not improve the maximum g-factor significantly (less than 3%). Therefore we chose the equivalent Tammes radius for all arrangements. The loop radii of each setup were 74.1 mm (8 channels), 53.7 mm (16 channels) and 39.2 mm (32 channels). In figure 3 we show maximum g-factor values for optimal (marker at bottom) and worst case (marker at top) coil arrangements. Clearly, keeping the acceleration fixed, with the number of channels increasing the difference between the optimal and worst case decreases. However for high acceleration with a low number of channels, an optimal coil arrangement relative to the acceleration directions is crucial. If we did 2x2 undersampling in k-space for example, an optimal arrangement of 8 loops resulted in a lower g_{\max} of 1.53 compared to 16 channels in bad configuration (1.75). Moreover in the case of having 16 channels, good loop arrangement offered similar PI performance at 3x3 acceleration ($g_{\max} = 1.72$) as with 2x2 undersampling arranged badly ($g_{\max} = 1.75$).

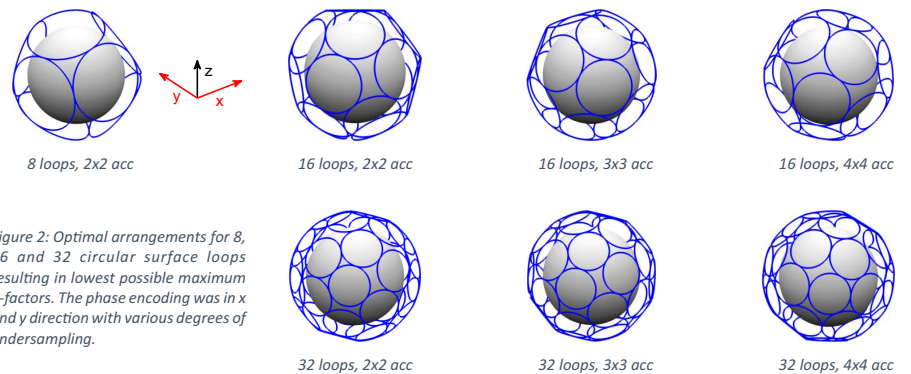
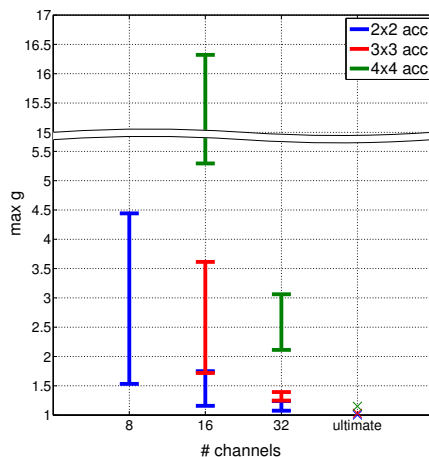


Figure 2: Optimal arrangements for 8, 16 and 32 circular surface loops resulting in lowest possible maximum g-factors. The phase encoding was in x and y direction with various degrees of undersampling.

Figure 3: Range of maximum g-factor for different number of channels and acceleration factors. Lower marker indicates optimal, upper worst arrangement.

Conclusion: If the number of receive channels is close to the undersampling rate in k-space positioning of circular surface coils with regard to the acceleration directions has significant influence on PI performance. Knowing the phase encoding direction(s) and undersampling rate in advance, we showed that our optimization approach fully exploited the unfolding skills for a given number of receivers.

References: [1] D. Sodickson, *MRM* 38, p. 591-603, 1997

[2] K. Pruessmann, *MRM* 42, p. 952-962, 1999 [3] M. Griswold, *MRM* 47, p. 1202-1210, 2002

[4] F. Wiesinger, *Parallel magnetic resonance imaging: potential and limitations at high fields*, Zürich, ETH, p. 61 ff., 2005

[5] R. Lattanzi *MRM* 68, p. 286-304, 2012

[6] L. Li, *IEEE Trans. Microwave Theory and Techniques* 42, p. 2302-2310, 1994

[7] R. Tammes, *Rec. Trav. Bot. Neerl.* 27, p. 1-84, 1930